JOURNAL OF BACTERIOLOGY, June 1986, p. 1046–1054
0021-9193/86/061046-09$02.00/0

Vol. 166, No. 3

Ultrastructure of the Cell Envelope of the Archaebacteria *Thermoproteus tenax* and *Thermoproteus neutrophilus*

PAUL MESSNER,[1]* DIETMAR PUM,[1] MARGIT SÁRA,[1] KARL O. STETTER,[2] AND UWE B. SLEYTR[1]

Zentrum für Ultrastrukturforschung, Universität für Bodenkultur, A-1180 Vienna, Austria,[1] and Lehrstuhl für Mikrobiologie, Universität Regensburg, D-8400 Regensburg, Federal Republic of Germany[2]

Received 25 October 1985/Accepted 22 January 1986

The ultrastructures of the regular surface layers (S-layers) of the extremely thermophilic archaebacteria *Thermoproteus tenax* and *Thermoproteus neutrophilus* were examined by freeze-etching, freeze-drying, and negative staining methods combined with optical and digital image enhancement. In both strains, a monolayer of macromolecules arranged in hexagonal arrays with center-to-center spacings of approximately 30 nm was the only component of the cell wall. The gross morphologies of the S-layer lattices of the two organisms were similar and showed the same handedness in the arrangement of the protomers of the morphological units. Striking differences were found in the anionic charge distributions on the surfaces of the two S-layer proteins as determined by labeling with polycationic ferritin. Analysis of the lattice orientation, together with the number and distribution of lattice faults on intact cells, provided a strong indication that the S-layers of both organisms have a shape-determining function.

Thermoproteus tenax (29) and *Thermoproteus neutrophilus* (6) are members of a recently discovered, novel order of extremely thermophilic anaerobic archaebacteria. They are hydrogen-sulfur autotrophic and grow at temperatures of up to 95°C (25). *T. tenax* differs from *T. neutrophilus* in that it can also grow heterotrophically and has an acidic pH growth optimum rather than one close to neutral (6). Their light microscopical appearance is that of extended aseptate rods of about 0.4 μm in diameter with a length of 1.0 to 80 μm. *T. tenax* often shows true branching (29). The bacteria are nonmotile and show a gram-negative staining reaction due to the simple wall architecture without a murein or pseudomurein layer (11, 12, 29). The walls consist of the cytoplasmic membrane and a hexagonally packed surface layer (S-layer) (22, 24).

We have investigated the ultrastructure and surface charge of *T. tenax* and *T. neutrophilus*, firstly to obtain information about proteins (13) which are able to withstand extreme environmental conditions and, secondly, to elucidate a possible morphogenetic function of S-layers in organisms in which paracrystalline arrays are the only component of the cell wall.

MATERIALS AND METHODS

Bacteria. *T. tenax* (DSM 2078) was isolated from a solfataric mud hole in the Kraffla area, Iceland. *T. neutrophilus* (DSM 2338) was isolated from a hot spring in the Kerlingarfjöll, Iceland. Both species were grown while stirred in Allen medium (1) supplemented with 0.5% sulfur and 0.02% yeast extract. The cultures were gassed with a mixture of 80% hydrogen and 20% carbon dioxide. *T. tenax* was grown at pH 5.5, and *T. neutrophilus* was grown at pH 6.8.

Materials. Cationized ferritin was purchased from Sigma Chemical Co., Munich, Federal Republic of Germany. All other chemicals used were of reagent grade.

Specimen preparation. For freeze-etching, the whole bacteria were centrifuged, and 1-μl samples were immediately frozen in Freon 22 (Polaron Equipment Ltd., Watford, England) kept close to its solidification temperature (−160°C). Freeze-etching was performed with a Balzers BA 360M freeze-etching unit (Balzers AG, Balzers, Liechtenstein) as described previously (16) with an etching time of 1.5 min at −98°C. For all other experiments, the samples were prepared as described below. Frozen bacteria (5 g) were suspended in 50 mM Tris hydrochloride buffer (pH 7.2; 40 ml) and were disrupted with a cell disintegrator (model B-15P; Branson Sonic Power Co., Danbury, Conn.) at maximum output for 5 min (16). The degree of disruption of the bacteria was checked by negative staining. The broken cells were centrifuged (model J2-21; Beckman Instruments, Fullerton, Calif.; 20,000 × *g*, 4°C, 20 min). Subsequently the crude envelope fragments, which formed the upper layer of the pellet, were carefully removed from the nondisrupted cells with a spatula. This purification procedure was repeated three times, and each step was checked by negative staining. The crude cell envelope preparations were combined, centrifuged, suspended in 0.5% Triton X-100–50 mM Tris hydrochloride buffer (2 ml) and incubated for 15 min at 80°C with stirring to solubilize the plasma membrane. After several washing steps with Tris hydrochloride buffer, the suspension was filtered (type 589/1 filter paper; Schleicher & Schuell, Dassel, Federal Republic of Germany) to remove residual sulfur from the culture medium. The filtrate was centrifuged and washed with Tris hydrochloride buffer. To disintegrate the cell wall sacculi into large monolayer fragments, the washed cell wall preparation was further sonicated for 2.5 min at maximum output. These suspensions were used for the following experiments.

For negative staining, grids coated with Formvar-carbon (Balzers AG) and rendered hydrophilic by glow discharge were floated for 2 min, facedown, on the surface of 1 drop of the suspension of either the cell wall sacculi or the monolayer fragments. Subsequently the samples were stained on 1 drop of a 1% uranyl acetate solution (pH 4.2) for 3 min. After removal of the excess stain by blotting with filter paper, the grids were air dried.

For freeze-drying, freshly prepared, carbon-coated copper grids (700 mesh) were floated for 10 min on 1 drop of the S-layer suspension. The grids were then blotted with a wet filter paper for ca. 45 s (14), and the unfixed samples were

* Corresponding author.

TABLE 1. Lattice parameters of purified S-layer fragments

Type of preparation	Surface location[a]	Center-to-center spacing (nm)	
		T. tenax (*n*)[b]	*T. neutrophilus* (*n*)[b]
Negative staining	—	30.4 ± 0.4 (41)	29.9 ± 0.8 (50)
Freeze-etched and shadowed	ES	31.4 ± 1.0 (50)	30.3 ± 0.9 (60)
Freeze-dried and shadowed	ES	31.2 ± 0.6 (47)	30.6 ± 0.9 (42)
	CS	31.4 ± 0.5 (61)	30.6 ± 0.5 (61)

[a] ES, Extracellular surface; CS, cytoplasmic surface; —, spacings measured on the monolayer.
[b] *n*, Number of measurements.

immediately frozen by plunging into liquid nitrogen. The frozen preparations were mounted under liquid nitrogen onto the precooled freeze-drying table of a Balzers BAF 300 freeze-etching machine and transferred into the unit by using the quick-loading device. After freeze-drying at −80°C for 2 h, the dehydrated samples were shadowed unidirectionally with a platinum-carbon layer (thickness, 1.0 nm) from an electron gun source with an elevation angle of 45°. The thickness of the layer was determined by using a quartz crystal monitor. The heavy metal shadow was reinforced with a carbon layer (thickness, 5 nm) deposited at an angle of 90° to the specimen surface.

Labeling experiments with polycationic ferritin (PCF) were performed for the cell wall suspensions at different pH values chosen to resemble the environmental conditions during growth of the two strains. After washing the S-layer preparations with distilled water to remove the Tris hydrochloride buffer, *T. tenax* samples (25 mg) were suspended in 0.5 ml of 0.1 M HCl-KCl buffer (pH 1.2), in 0.1 M glycine hydrochloride buffer (pH 2.2), or in distilled water (pH 5.7). *T. neutrophilus* was treated only in distilled water (pH 5.7). An excess of PCF (2 drops of the sterile solution, 10.4 mg of ferritin ml^{-1}) was added to each suspension, and the suspensions were incubated for 10 min at room temperature. Unreacted marker was removed by repeated washing with distilled water, and the samples were then used for freeze-drying or negative staining experiments. The net charge of the surface of the native S-layer fragments could be changed by blocking the amino groups of the proteins with glutaraldehyde. Pellets of cell envelopes of both strains were washed in distilled water to remove residual Tris hydrochloride buffer and suspended in 0.5% glutaraldehyde–0.1 M cacodylate buffer (pH 7.2) for 20 min at room temperature. Unreacted fixative was removed by several washes with distilled water. These preparations were then labeled with PCF as described for nonfixed specimens.

Electron microscopy. The specimens were investigated in an electron microscope (model EM 301; Philips, Eindhoven, The Netherlands), equipped with a liquid nitrogen anticontamination device, and operated at 80 kV. A 30-μm objective aperture was used, and the micrographs were recorded at a nominal magnification of ×25,000 on Agfa Scientia 23D56 film (Agfa-Gevaert, Leverkusen, Federal Republic of Germany) for image processing or on Kodak 5302 film (Eastman Kodak Co., Rochester, N.Y.). The magnification was calibrated by using negatively stained catalase crystals (28).

Image processing. The micrographs were screened by optical diffraction with a DeRosier-type diffractometer (19) constructed in this laboratory. Those regions which were preserved to a resolution better than 4 nm (eighth-order reflections) were selected for subsequent computer image reconstructions. The noise spectrum was examined to ensure that astigmatism was negligible and the first minimum of the phase contrast transfer function was at a frequency substantially higher than the highest frequency diffraction spots. The micrographs were scanned with a microdensitometer (model C 4500; Optronics International Corp., Chelmsford, Mass.) or a flatbed microdensitometer (model PDS; Perkin Elmer Corp., Garden Grove, Calif.) with a raster spacing corresponding to approximately 0.8 nm on the original object. Areas of 256 by 256 or 512 by 512 picture elements were used for the analysis. At least 20 different images of both negatively stained and freeze-dried preparations were used for the analysis. The digitized images were processed by using both Fourier domain methods and correlation averaging (21). Amplitudes and phases of the diffraction maxima were interpolated with the use of a peak profile-fitting procedure (15, 18) from images with good long-range order. Symmetry-related pairs were complex averaged (15). Only motifs with a minimum of strain were used for the real-space averaging. Motifs were rejected from the summation when their root mean square displacement change from the neighbors (normalized with respect to the base vector length) exceeded a value of 0.05 (O. W. Saxton, personal communication). Processed data were output as continuous tone images on the Optronics C 4500 Photomation system. Variations within images of the two S-layers and variations within the same layer, depending on the orientation of adsorption, were tested. The statistical significance of the differences of the sets of Fourier terms was determined by using the two-sample *t* test (BMDP Statistical Software 1981, option Hotelling T^2, Dept. of Biomathematics, University of California, Los Angeles).

RESULTS

Morphology and lattice parameters of the crystalline S-layers. Freeze-etching was used to demonstrate the surface features of the native cell walls of *T. tenax* (Fig. 1a) and *T. neutrophilus* (Fig. 1b). The hexagonal S-layer lattices found on both organisms showed a characteristic orientation with one lattice vector running perpendicular to the longitudinal axis of the cell. Independent of the shadowing direction, the freeze-etch images of the two S-layer lattices revealed slight differences. The lattice constants derived from the freeze-etch preparations of intact cells and measurements on negatively stained or freeze-dried S-layer preparations are summarized in Table 1. Evaluation by the *t* test did not show statistically significant differences.

Isolated S-layer sacculi of both strains examined by negative staining (Fig. 2c and f) revealed Moiré patterns originating from the two superimposed wall layers of the flattened cylindrical cell envelope. The edge-on views (Fig. 2a and d) gave some indications that the protein of the S-layer sacculi

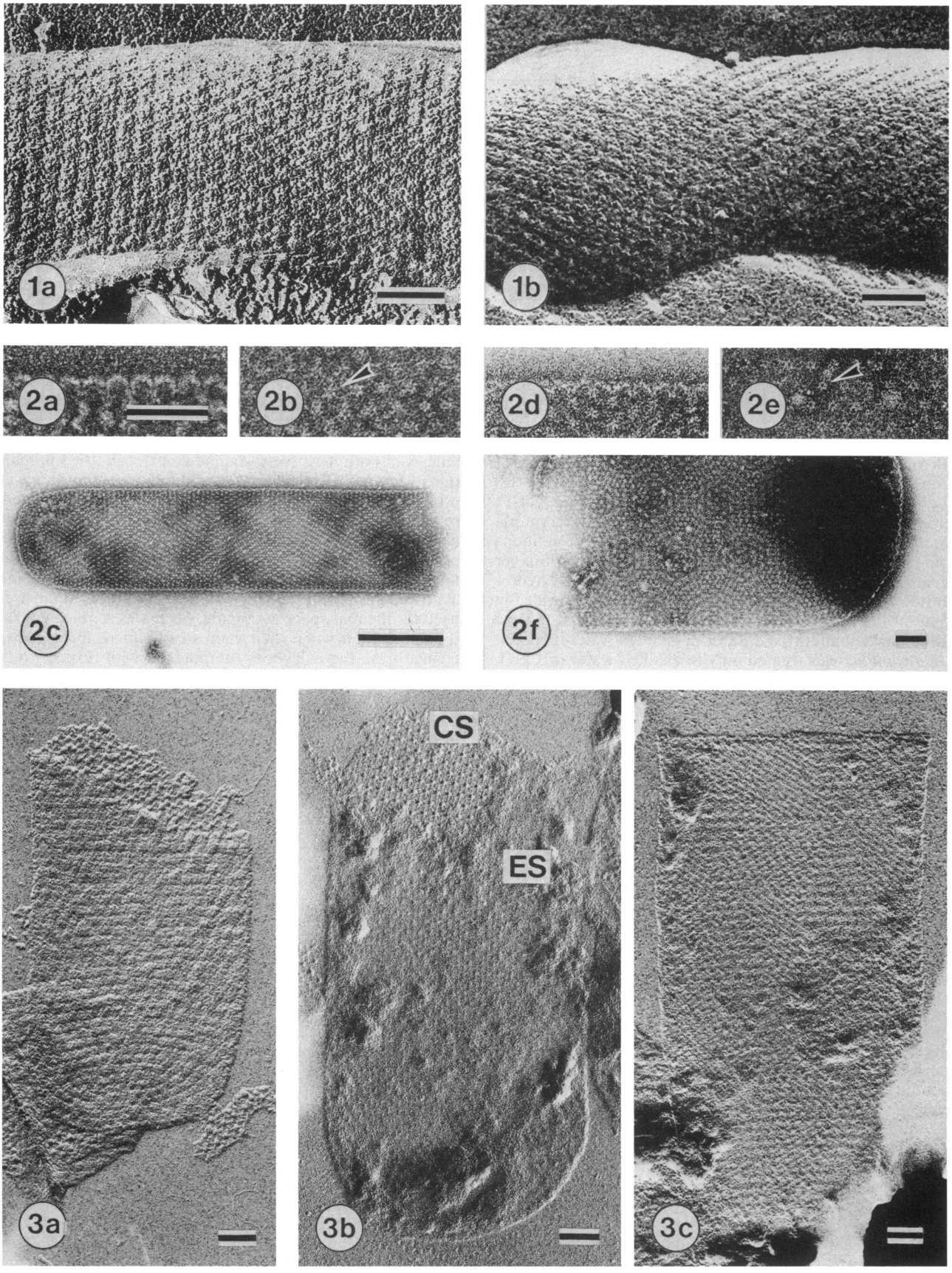
1a
1b
2a
2b
2d
2e
2c
2f
CS
ES
3a
3b
3c

protruded toward the cytoplasmic side, while the outer surface appeared less sculptured. In both S-layers, stain-filled channels seemed to traverse the structure. Monolayers of the sacculi reveal a hexagonal arrangement of starlike structures (Fig. 2b and e, arrows). The starlike morphological units of *T. neutrophilus* differed from those of *T. tenax* by showing a higher stain density in the central region.

Freeze-dried and shadowed preparations of S-layer sacculi of both strains (Fig. 3a and b) revealed characteristic differences in the topographies of the inner and outer surfaces. While the outer side of the layers appeared relatively smooth, the inner surface was highly sculptured. The dominant topographical features seen on the inner side of the sacculi of both organisms were dome-shaped protrusions which had diameters similar to those of the starlike structures seen in the negative staining preparations (Fig. 2b and e). The latter appeared more sharply defined in *T. neutrophilus* (Fig. 3b) than in *T. tenax* (Fig. 3a). As already observed to some extent on images of freeze-etched preparations, the two S-layers revealed differences in the fine structure of their extracellular surface after freeze-drying and high-resolution shadowing. While the freeze-dried surface of *T. tenax* was comparable to that of the freeze-etching result (Fig. 1a), the characteristic S-layer topography seen on freeze-etched *T. neutrophilus* cells (Fig. 1b) seemed to disappear during freeze-drying. Moiré patterns comparable to those of negatively stained specimens (Fig. 2f) became visible on preparations of collapsed cylindrical envelopes (Fig. 3b and c). Presumably, the tips of the dome-shaped particles on the inner side of the S-layer caused elevations on the surface of the superimposed layer. Preparations of *T. neutrophilus* always contained remnants of cytoplasmic material which could not be removed by using the same purification procedure as that applied to *T. tenax*. The widths of the flattened sacculi of *T. neutrophilus* varied from 480 to 630 nm, giving an average diameter for the cylindrical cell body of ca. 350 nm.

Labeling with PCF. *T. neutrophilus* labeled with PCF at pH 5.7 (pH of the distilled water) yielded a random distribution of the PCF marker on the extracellular surface of the S-layer (Fig. 4a), while the inner side did not bind PCF (Fig. 4b). After treatment of the S-layer of *T. neutrophilus* with glutaraldehyde, which interacts with the free amino groups of the protein, the binding properties of the outer surface did not change, but the inner side appeared completely covered with ferritin molecules (not shown).

T. tenax exhibited random binding of the PCF marker at pH 1.2, which was not different from the glow-discharged carbon layer (not shown), but showed a significant labeling at pH 2.2 (Fig. 5). When labeling was performed at pH 5.7, PCF bound to the outer surface in a regular fashion (Fig. 6 and 7a and b) at distances identical with the center-to-center spacing of the morphological units of the S-layer lattice (Table 1). The hexagonal lattice generated by the bound PCF molecules revealed the same orientation as the unlabeled S-layer, with one axis perpendicular to the longitudinal axis of the collapsed cylinder. As opposed to the extracellular surface, the cytoplasmic surface of the S-layer only bound PCF in a random, dense layer (not shown). Dislocations, as observed in many S-layers (8, 22, 23), could not be found in the cylindrical regions of the sacculi.

Because one PCF molecule was bound per morphological unit of the S-layer lattice (see Fig. 9), lattice faults in the cell envelope preparations became clearly visible (Fig. 7a and b). In crystallographic terms, these lattice faults can be described as local wedge disclinations (9). By evaluating the locations and distances of the wedge disclinations on more than 25 freeze-dried preparations of PCF-labeled cell poles, the presence of six disclinations per cell pole could be calculated. This is in agreement with the theoretical considerations of Caspar and Klug (3) who suggested that a closed protein container could be constructed from identical units quasiequivalently bonded into a large number of six-coordinated units together with 12 five-coordinated units (either pentamers or randomly bonded hexamers). S-layers of *T. tenax* treated with glutaraldehyde showed the same binding characteristics for PCF molecules as did unfixed cell envelopes labeled at pH 5.7 (not shown).

Image analysis of the cell envelopes. Monolayer fragments of the S-layer sacculi, obtained by sonication, were used for image reconstruction analyses of negatively stained specimens. Characteristic optical diffraction patterns of areas selected for computer reconstruction are shown in Fig. 8b, e, h, and k. Reflections in the computed diffraction patterns (not shown) down to a resolution of 2.2 nm were still accepted by the phase criterion (17) and therefore were used in the reconstruction procedures.

S-layers of both strains gave quite similar but statistically significant different ($P = 0.99$) filtered images when adsorbed so that the cystoplasmic surface was adjacent to the carbon supporting layer (Fig. 8a and g). The two-dimensional projections showed well-defined stain-protein boundaries with sharp gradients of density. The bulk of the protein was arranged around the sixfold axis with center-to-center spacings of approximately 30 nm (Table 1) and consisted of six identical units which formed a paddle-wheel-like structure with the same characteristic handedness for both strains. A smaller proportion of protein accumulated on the axes with threefold symmetry between the major protein complexes. Narrow bridges interconnected the proteins on the six- and threefold axes and thus formed a network with large, stain-filled cavities in between. Negatively stained S-layers of *T. tenax* revealed a low stain density in the central area of the bulk protein arranged around the sixfold axis (Fig. 8a), whereas the density was high in the corresponding region of envelope preparations of *T. neutrophilus* (Fig. 8g). When adsorbed with the extracellular surface against the supporting layer, the envelopes of *T. tenax* revealed a similar but statistically significant different ($P = 0.99$) stain exclusion pattern (Fig. 8d) compared with that observed after adsorption with the cytoplasmic side (Fig. 8a). More stain was accumulated in the central region on the sixfold axis, and the protein on the threefold axis looked unstained, but the regions of high stain density between the major protein complexes maintained their general appearance and dimensions. A distinctly different image was obtained from *T.*

FIG. 1. Electron micrographs of freeze-etched preparations of *T. tenax* (a) and *T. neutrophilus* (b). Bars, 100 nm.

FIG. 2. Negatively stained preparations of envelopes of *T. tenax* (a through c) and *T. neutrophilus* (d through f). Edge-on views are shown of folded envelopes (a and d), monolayer fragments (b and e; arrows point to starlike morphological units), and envelope fragments obtained by ultrasonication of intact cells (c and f). Panels a, b, d, and e have identical magnifications (bars, 100 nm). Bar in panel c, 500 nm.

FIG. 3. Freeze-dried and platinum-carbon-shadowed envelope preparations of *T. tenax* (a) and *T. neutrophilus* (b and c). CS, Cytoplasmic surface; ES, extracellular surface. Bars, 100 nm.

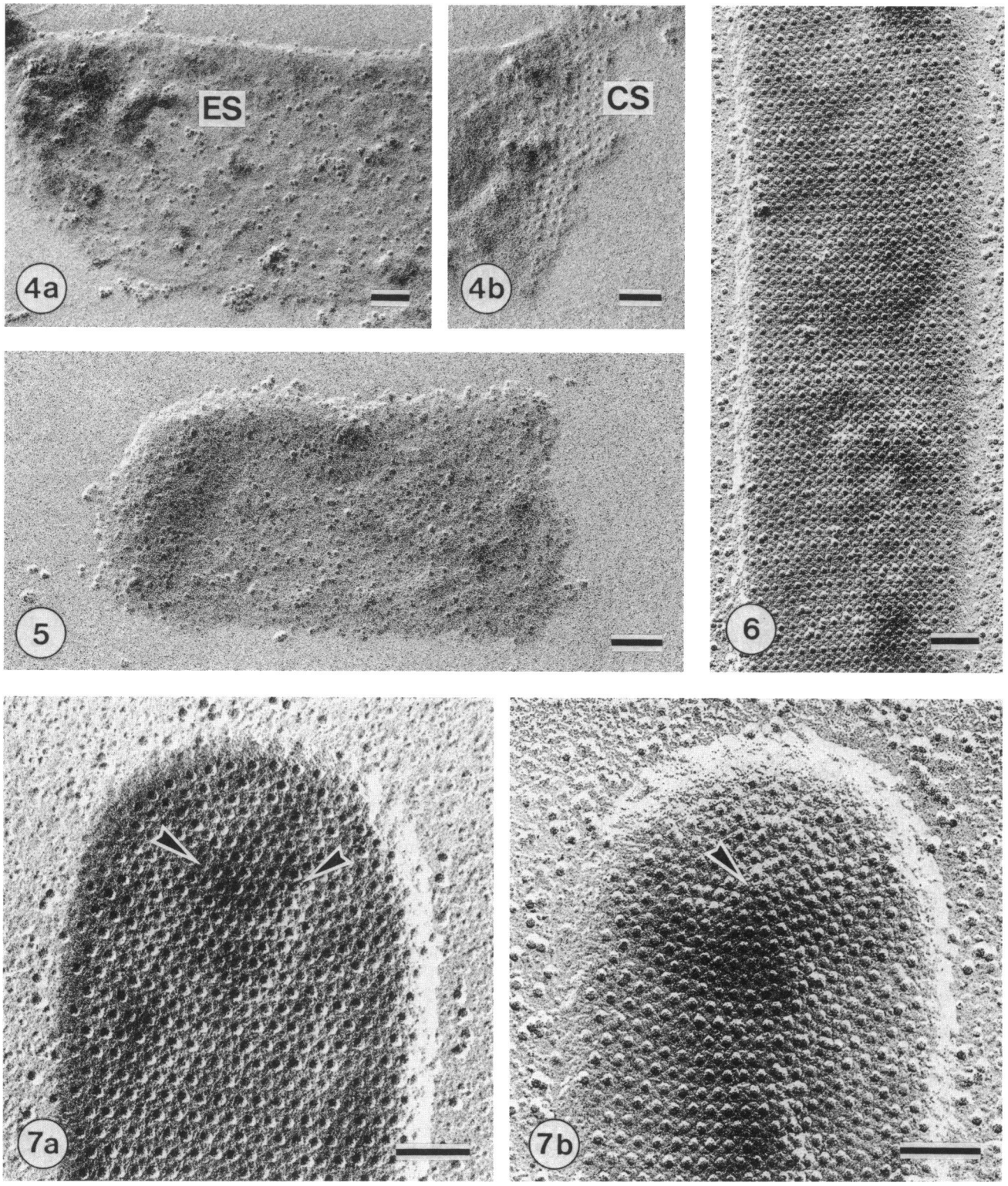

FIG. 4. Freeze-dried and shadowed preparations of envelopes of *T. neutrophilus* labeled at pH 5.7 with PCF. Extracellular surface (ES) (a) and cytoplasmic surface (CS) (b). PCF binds to the extracellular surface in a random fashion but no PCF is adsorbed to the cytoplasmic surface.

FIG. 5. Freeze-dried and shadowed preparation of envelopes of *T. tenax* labeled at pH 2.2 with PCF, showing a random adsorption of PCF.

FIG. 6. Freeze-dried and shadowed preparation of envelopes of *T. tenax* labeled at pH 5.7 with PCF. The marker binds to the extracellular surface in a regular fashion.

FIG. 7. Preparation as described in the legend to Fig. 6. Arrows indicate positions of two (a) or one (b) local wedge disclinations in the lattice. Bars, 100 nm.

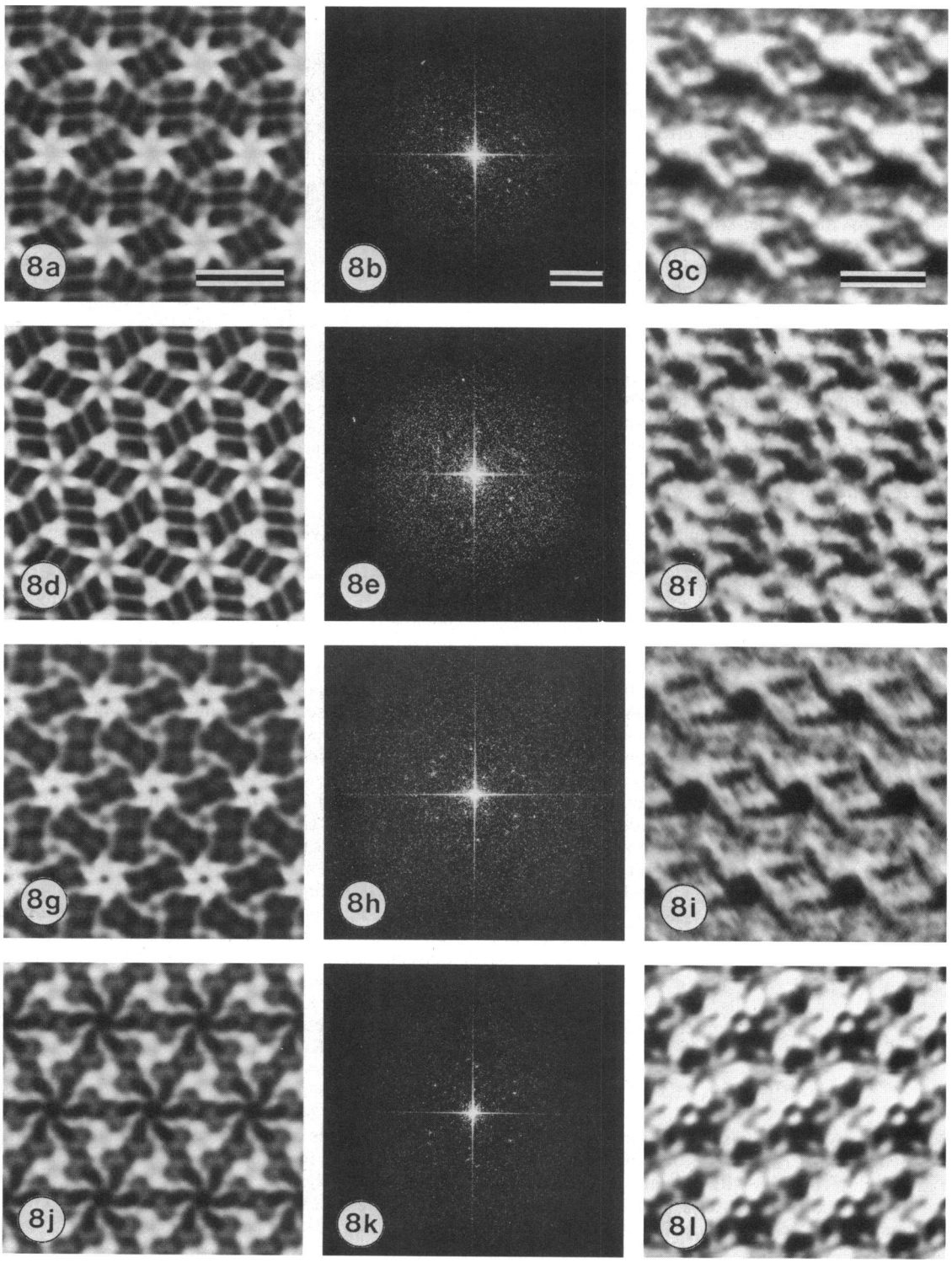

FIG. 8. Computer image reconstruction (a, c, d, f, g, i, j, and l) and optical diffraction patterns (b, e, h, and k) of *T. tenax* (a, b, d, and e) and *T. neutrophilus* (g, h, j, and k). Image reconstructions (a, d, g, and j) and optical diffraction patterns were derived from negatively stained envelope layer fragments. Reconstructed images of freeze-dried and shadowed envelopes of *T. tenax* (c and f) and *T. neutrophilus* (i and l). Images were derived from envelope preparations adsorbed with the cytoplasmic surface to the supporting layer (a through c and g through i). Envelopes were adsorbed with the extracellular surface (d through f and j through l). Bars in computer image reconstruction, 25 nm; bar, in the diffractograms, 0.2 nm^{-1}.

neutrophilus envelopes after adsorption with the extracellular surface against the supporting layer (Fig. 8j) compared with that of adsorption with the opposite surface (Fig. 8g). The conspicuous features were dominant stain-filled indentations between the arms of the paddle-wheel-like structures, so dominant that the latter seemed to disappear. The region of the threefold axes seemed to be less stained. The stain accumulations at the center of the sixfold axes seen on *T. neutrophilus* envelope fragments after adsorption with either surface against the supporting layer (Fig. 8g and j) led to the assumption that there was a stain-filled pore penetrating the protein complex (Fig. 2d).

The handedness of the paddle-wheel-like structure of the main protein complex was determined from freeze-dried and shadowed specimens of both strains with known orientation in the microscope. When viewed from above, the arms of the paddle-wheel-structures of both strains showed a right-handed curvature (Fig. 8c and i). The prominent topographical features were the protruding paddle-wheel-like domains. Parallel depressions which correlated with the positions of the stain-filled cavities in negatively stained preparations (Fig. 8a and g) surrounded the major protein domains. Depending on the shadowing geometry, the appearance of some structural details was limited by a self-shadowing effect. Compared with those of *T. neutrophilus* (Fig. 8i), the protein domains on the threefold axes of *T. tenax* preparations (Fig. 8c) were more easily distinguished.

As already observed, the filtered images of the freeze-dried and shadowed extracellular surfaces of S-layer sacculi of both strains (Fig. 8f and l) revealed a similar unsculptured appearance in edge-on views of negatively stained envelopes (Fig. 2a and d). In both strains, the domains of the protein protrusions on the threefold axes were the dominant features of the surface. Instead of the paddle-wheel-like protrusions of the main protein complex, as were present on the cytoplasmic side of envelope preparations of both strains, less prominent hexagonal arrangements of proteins were visible on the extracellular surface (Fig. 8f and l). Characteristic circular depressions could be seen in the center of the major protein complexes. The parallel depressions seen on the cytoplasmic side of the S-layer sacculi of both strains (Fig. 8c and i) were not easily seen on the extracellular surface.

Image processing of freeze-dried and shadowed preparations of PCF-labeled envelopes of *T. tenax* revealed that the marker molecules were bound in the position of the sixfold axes because each ferritin molecule was surrounded by six protein domains (Fig. 9). Depending on the shadowing direction, some structural details of the protein network between the three- and sixfold symmetry axes were visible.

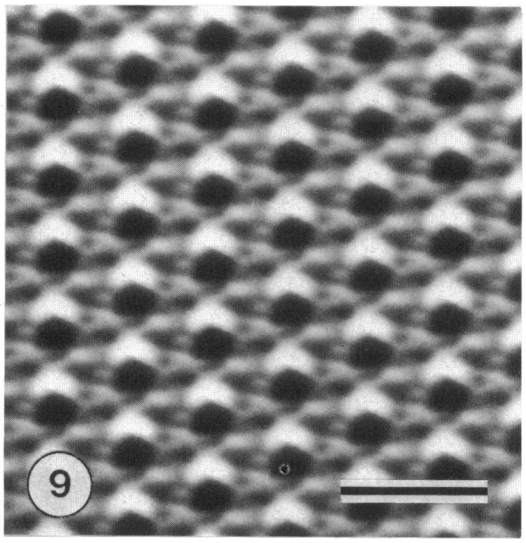

FIG. 9. Computer image reconstruction of PCF-labeled, freeze-dried, and shadowed envelope preparations of *T. tenax* (as described in the legend to Fig. 6). The marker molecules are located in the positions of the sixfold-symmetry axes. Bar, 50 nm.

DISCUSSION

The crystalline S-layers on the surface of intact cells of *T. tenax* and *T. neutrophilus* revealed lattices with p6 symmetry having morphological units with similar center-to-center spacings. Although many eubacteria and archaebacteria possess hexagonally ordered S-layers (24; U. B. Sleytr, P. Messner, M. Sára, and D. Pum, System. Appl. Microbiol., in press), the mass distribution of the two S-layers described here revealed unique features that have not, so far, been observed in other bacteria. Negatively stained preparations of S-layer envelopes show areas with high stain density, which suggests that they are traversed by pores (24, 26). In contrast to the hexagonal arrays on *Sulfolobus acidocaldarius* (5, 27), no large central pores in the main protein complexes have been found in the S-layers of either *Thermoproteus* strain.

In both organisms, the prominent structural complexes at the axes of sixfold symmetry of the side facing the cytoplasmic membrane were responsible for the rough appearance of the inner side of the S-layer sacculi. The outer surfaces of both envelopes looked relatively smooth, and this same feature, of smooth outer surface but rough inner face, has also been observed frequently on other S-layers, e.g., *Aquaspirillum serpens* (7), *Deinococcus radiodurans* (2), *Chlamydia trachomatis* (4), or *Sulfolobus acidocaldarius* (5).

T. tenax and *T. neutrophilus* are able to grow at temperatures up to 95°C and, in the case of *T. tenax*, at highly acidic pH. These facts reflect the highly stable nature of the S-layer proteins which maintain their structural integrity even under extreme environmental conditions. All attempts to disintegrate the crystalline protein matrices into subunits have so far failed, due, no doubt, to their remarkable resistance to dissociation by high temperature, chemical treatment (e.g., boiling in detergents, acids, and bases), and mechanical disruption (H. König, personal communication).

Thin sections of cells of both *T. tenax* (29) and *T. neutrophilus* (König, personal communication) have shown that the S-layers are the only cell wall component. Further, S-layers generally contain a high proportion of hydrophobic amino acids (24). It would be interesting to investigate whether the tips of the protrusions on the cytoplasmic side of the sacculi are hydrophobic or hydrophilic. If hydrophobic, they might anchor the envelope protein into the hydrophobic lipid matrix of the cytoplasmic membrane, while, if hydrophilic, they could act as spacers between the hydrophilic surface of the plasma membrane and the S-layer proper. In either case, relatively free lateral diffusion of a considerable amount of membrane lipids and proteins between the linkage points would be ensured.

From the two-dimensional information provided by image reconstructions of negatively stained envelope samples, we cannot describe the shape of the subunits with precision. However, the stain exclusion pattern favors an arrangement

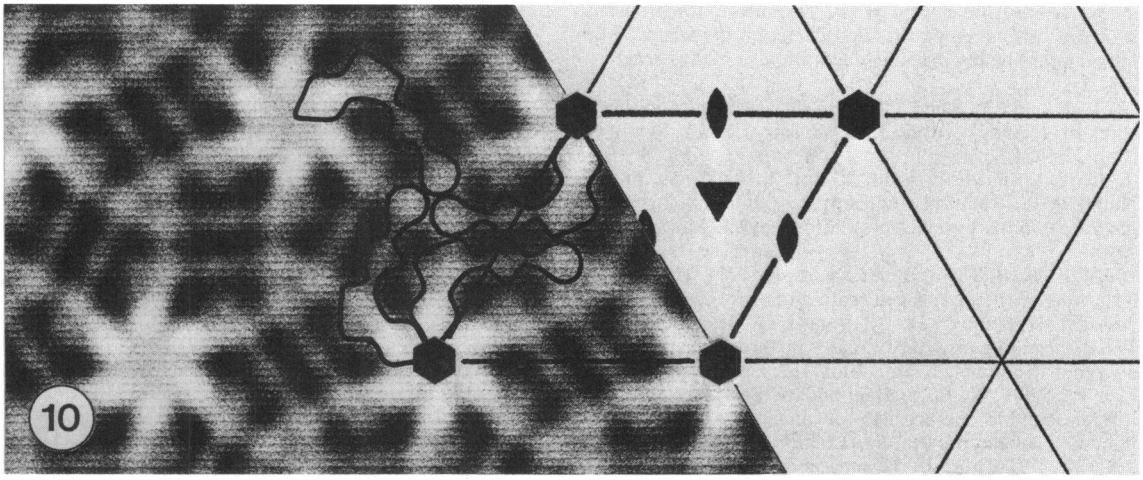

FIG. 10. Computer image reconstruction of negatively stained envelope of *T. tenax* (equivalent to Fig. 8a) with corresponding unit cell and positions of the symmetry axes. The contours of the protomers are arbitrary but represent the simplest possible molecular shape.

derived from a single, bent proteinaceous subunit (Fig. 10). The contribution of this single subunit to the formation of the structural complexes on a sixfold axis and an adjacent threefold axis would yield a closely interlocked S-layer network which could provide a rigid rod-like cell structure. The morphologies of both organisms are similar to those of other rod-shaped bacteria which do have rigid wall components. The lattice orientations were well defined and identical in the two strains, and no dislocations have so far been found on the cylindrical parts of the cells. From a theoretical point of view, the shape of both bacteria can be regarded as cylinders closed by two hemispherical caps. To cover such a surface with a continuous hexagonal array, no lattice fault would be required for the cylindrical part. However, at least six pentameric units would be needed to provide a continuous coverage over each hemispherical pole (3, 5). The radius of curvature and, therefore, the diameter of the cell would be determined by the mass distribution and bonding properties of the individual protomeric units. Elongation of the cylindrical part of the cell would most probably involve incorporation of protomeric subunits at sites of sliding dislocations (9). From the PCF labeling experiment on *T. tenax*, it was possible to demonstrate such predicted lattice faults at the cell poles, but we have been unable to distinguish whether the dislocations originated from pentamers or from randomly bound hexamers. S-layers are the exclusive wall component in both organisms, and both organisms have a well-defined rodlike morphology. We therefore conclude that this evidence provides, for the first time, strong support for the notion that S-layers can play a major role in the determination of cell shape, as predicted by Henning and Schwarz (10).

Despite the considerable morphological similarities of the two organisms, distinct differences exist in the net surface charges of the native S-layer proteins. Depending on the pH conditions, the inner and outer surfaces of the envelope preparations of the two strains showed different binding patterns. This variation could arise from two sources. Firstly, carboxyl groups, as donors of negative charges, could dissociate, and also the accessibility of negatively charged groups on the surface could change as a result of modified protein conformation in relation to variation of pH. Secondly, it is probable that the amino acid sequences of the S-layers of *T. tenax* and *T. neutrophilus* are different. Similar arguments could be used to explain the differences seen in the structural preservation of the morphological details of envelope preparations of the two strains after freeze-drying. Less structural collapse was seen in *T. tenax* envelopes compared with *T. neutrophilus* envelopes after flattening of the proteins onto the supporting layer.

As with other bacterial cell wall surface structures, S-layers have most probably evolved as a consequence of interactions between the cells and their environment. They could therefore have a barrier function against both external and internal factors (24). The pore size for both strains is about 6 nm, as suggested by the stain exclusion patterns of envelope preparations. This would be in the range of pore sizes determined from permeability studies (20; U. B. Sleytr and M. Sára, Gesellsch. Biotechnol. Forsch. monogr., in press), which have shown that the nominal molecular weight cutoff (i.e., a 90% retention of a particular molecule of known molecular weight) of S-layers of both strains is ca. 67,000. Similar values have been obtained from *Sulfolobus acidocaldarius* S-layer preparations (20; Sleytr and Sára, in press) where the permeability properties could be compared with the three-dimensional model of the S-layer protein derived from high-resolution electron microscopy (5). Thus, although our estimate of pore size is based only on results from the two-dimensional studies, we feel that, together, these considerations support our view that the effective pore size is probably close to 6 nm.

Now that structural details of the walls of these archaebacteria have been described, our understanding of their functional morphology can be augmented by further biochemical work and determination of the subunit linkage strengths between the cell wall components.

ACKNOWLEDGMENTS

We thank A. W. Robards for critical reading of the manuscript.

This work was supported by grants from the Österreichischer Fonds zur Förderung der wissenschaftlichen Forschung, Projekt 4613 and 5290, and the Deutsche Forschungsgesellschaft, SFB 43.

LITERATURE CITED

1. **Allen, M. B.** 1959. Studies with *Cyanidium caldarium*, an anomalously pigmented chlorophyte. Arch. Mikrobiol. **32:** 270–277.

2. **Baumeister, W., O. Kübler, and H. P. Zingsheim.** 1981. The structure of the cell envelope of *Micrococcus radiodurans* as revealed by metal shadowing and decoration. J. Ultrastruct. Res. **75**:60–71.
3. **Caspar, D. L. D., and A. Klug.** 1962. Physical principles in the construction of regular viruses. Cold Spring Harbor Symp. Quant. Biol. **27**:1–24.
4. **Chang, J. J., K. Leonard, T. Arad, T. Pitt, Y. X. Zhang, and L. H. Zhang.** 1982. Structural studies of the outer envelope of *Chlamydia trachomatis* by electron microscopy. J. Mol. Biol. **161**:579–590.
5. **Deatherage, J. F., K. A. Taylor, and L. A. Amos.** 1983. Three-dimensional arrangement of the cell wall protein of *Sulfolobus acidocaldarius*. Appendix: D. A. Agard, A least-squares method for determining structure factors in three-dimensional tilted-view reconstructions. J. Mol. Biol. **167**:823–852.
6. **Fischer, F., W. Zillig, K. O. Stetter, and G. Schreiber.** 1983. Chemolithoautotrophic metabolism of anaerobic extremely thermophilic archaebacteria. Nature (London) **301**:511–513.
7. **Glaeser, R. M., W. Chiu, D. Grano, and K. Taylor.** 1980. Morphological model of the surface-layer array in *Spirillum serpens*, p. 22–26. *In* W. Baumeister and W. Vogell (ed.), Electron microscopy at molecular dimensions. Springer-Verlag, Berlin.
8. **Harris, W. F.** 1977. Disclinations. Sci. Am. **237**:130–145.
9. **Harris, W. F., and L. E. Scriven.** 1970. Function of dislocations in cell walls and membranes. Nature (London) **228**:827–829.
10. **Henning, U., and U. Schwarz.** 1973. Determinants of cell shape, p. 413–438. *In* L. Leive (ed.), Bacterial membranes and walls. Marcel Dekker, Inc., New York.
11. **Kandler, O.** 1982. Cell wall structures and their phylogenetic implications. Zentralbl. Bakteriol. Hyg. 1 Abt. Orig. C **3**:149–160.
12. **Kandler, O., and H. König.** 1978. Chemical composition of the peptidoglycan-free cell walls of methanogenic bacteria. Arch. Microbiol. **118**:141–152.
13. **Kandler, O., and H. König.** 1985. Cell envelopes of archaebacteria, p. 413–457. *In* C. R. Woese and R. S. Wolfe (ed.), The bacteria, vol. VIII. Archaebacteria. Academic Press, Inc., New York.
14. **Kistler, J., U. Aebi, and E. Kellenberger.** 1977. Freeze drying and shadowing a two-dimensional periodic specimen. J. Ultrastruct. Res. **59**:76–86.
15. **Kübler, O.** 1980. Unified processing for periodic and nonperiodic specimens. J. Microsc. Spectrosc. Electron. **5**:561–575.
16. **Messner, P., F. Hollaus, and U. B. Sleytr.** 1984. Paracrystalline cell wall surface layers of different *Bacillus stearothermophilus* strains. Int. J. Syst. Bacteriol. **34**:202–210.
17. **Pum, D., and O. Kübler.** 1984. Comparative analysis of periodic structures with Fourier transform processing and correlation averaging. Proc. Eur. Congr. Electron Microsc. Budapest **2**:1331–1340.
18. **Roberts, K., P. J. Shaw, and G. J. Hills.** 1981. High-resolution electron microscopy of glycoproteins: the crystalline cell wall of *Lobomonas*. Appendix: P. J. Shaw, A peak profile analysis procedure for extracting unit cell transform data from the Fourier transforms of periodic arrays. J. Cell Sci. **51**:295–321.
19. **Salmon, E. D., and D. DeRosier.** 1981. A surveying optical diffractometer. J. Microsc. **123**:239–247.
20. **Sára, M., and U. B. Sleytr.** 1985. Verwendung isoporer, kristalliner Bakterienzellwandschichten als Ultrafiltrationsmembranen. Lebensm. Biotechnologie. **4**:141–146.
21. **Saxton, W. O., and W. Baumeister.** 1982. The correlation averaging of a regularly arranged bacterial cell envelope protein. J. Microsc. **127**:127–138.
22. **Sleytr, U. B.** 1978. Regular arrays of macromolecules on bacterial cell walls: structure, chemistry, assembly, and function. Int. Rev. Cytol. **53**:1–64.
23. **Sleytr, U. B., and A. M. Glauert.** 1975. Analysis of regular arrays of subunits on bacterial surfaces; evidence for a dynamic process of assembly. J. Ultrastruct. Res. **50**:103–116.
24. **Sleytr, U. B., and P. Messner.** 1983. Crystalline surface layers on bacteria. Annu. Rev. Microbiol. **37**:311–339.
25. **Stetter, K. O., and W. Zillig.** 1985. *Thermoplasma* and the thermophilic sulfur-dependent archaebacteria, p. 85–170. *In* C. R. Woese and R. S. Wolfe (ed.), The bacteria, vol. VIII. Archaebacteria. Academic Press, Inc., New York.
26. **Stewart, M., and T. J. Beveridge.** 1980. Structure of the regular layer of *Sporosarcina ureae*. J. Bacteriol. **142**:302–309.
27. **Taylor, K. A., J. F. Deatherage, and L. A. Amos.** 1982. Structure of the S-layer of *Sulfolobus acidocaldarius*. Nature (London) **299**:840–842.
28. **Wrigley, N. G.** 1968. The lattice spacing of crystalline catalase as an internal standard of length in electron microscopy. J. Ultrastruct. Res. **24**:454–464.
29. **Zillig, W., K. O. Stetter, W. Schäfer, D. Janekovic, S. Wunderl, I. Holz, and P. Palm.** 1981. *Thermoproteales*: a novel type of extremely thermoacidophilic anaerobic archaebacteria isolated from Icelandic solfataras. Zentralbl. Bakteriol. Hyg. 1 Abt. Orig. C **2**:205–227.